

Crete - 97/14

A Statistic for the Detection of Long Strings in Microwave Background Maps.

Leandros Perivolaropoulos

Department of Physics, University of Crete, 71003 Heraclion, GREECE

Received _____; accepted _____

ABSTRACT

Using analytical methods and Monte Carlo simulations, we analyze a new statistic designed to detect isolated step-like discontinuities which are coherent over large areas of Cosmic Microwave Background (CMB) pixel maps. Such coherent temperature discontinuities are predicted by the *Kaiser-Stebbins* effect to form due to long cosmic strings present in our present horizon. The background of the coherent step-like seed is assumed to be a scale invariant Gaussian random field which could have been produced by a superposition of seeds on smaller scales and/or by inflationary quantum fluctuations. The effects of uncorrelated Gaussian random noise are also considered. The statistical variable considered is the Sample Mean Difference (SMD) between large neighbouring sectors of CMB maps, separated by a straight line in two dimensional maps and a point in one dimensional maps. We find that including noise, the SMD statistics can detect *at the 1σ to 2σ level* the presense of a long string with $G\mu(v_s\gamma_s) = \frac{1}{8\pi}(\frac{\delta T}{T})_{rms} \simeq 0.5 \times 10^{-7}$ while more conventional statistics like the skewness or the kurtosis require a value of $G\mu$ *almost an order of magnitude larger* for detectability at a comparable level.

Subject headings: cosmic microwave background - cosmic strings

1. Introduction

The major progress achieved during the past 15 years in both theory and cosmological observations has turned the search for the origin of cosmic structure into one of the most exciting fields of scientific research (for a good review see Efstathiou 1989). Despite the severe constraints imposed by detailed observational data on theories for structure formation the central question remains open: *What is the origin of primordial fluctuations that gave rise to structure in the universe?* Two classes of theories attempting to answer this question have emerged during the past ten years and have managed to survive through the observational constraints with only minor adjustments.

According to the first class, primordial fluctuations are produced by quantum fluctuations of a linearly coupled scalar field during a period of inflation (Hawking 1982; Starobinsky 1982; Guth & Pi 1982; Bardeen, Steinhardt & Turner 1983). These fluctuations are subsequently expected to become classical and provide the progenitors of structure in the universe. Because of the extremely small linear coupling of the scalar field, needed to preserve the observed large scale homogeneity, the inflationary perturbations are expected by the central limit theorem, to obey Gaussian statistics. This is not the case for the second class of theories.

According to the second class of theories (Kibble 1976; Vilenkin 1981; Vilenkin 1985; Turok 1989; Brandenberger 1992; Perivolaropoulos 1994), primordial perturbations are provided by *seeds* of trapped energy density produced during symmetry breaking phase transitions in the early universe. Such symmetry breaking is predicted by Grand Unified Theories (GUT's) to occur at early times as the universe cools and expands. The geometry of the produced seeds, known as *topological defects* is determined by the topology of the vacuum manifold of the physically realized GUT. Thus the defects may be pointlike (monopoles), linelike (cosmic strings), planar (domain walls) or collapsing pointlike

(textures).

The cosmic string theory (Vilenkin 1981) for structure formation is the oldest and (together with textures (Turok 1989)) best studied theory of the topological defect class. By fixing its single free parameter $G\mu$ (μ is the *effective* mass per unit length of the wiggly string and G is Newtons constant) to a value consistent with microphysical requirements coming from GUT's, the theory may automatically account for large scale filaments and sheets (Vachaspati 1986; Stebbins *et. al.* 1987; Perivolaropoulos, Brandenberger & Stebbins 1990; Vachaspati & Vilenkin 1991; Vollick 1992; Hara & Miyoshi 1993), galaxy formation at epochs $z \sim 2 - 3$ (Brandenberger *et. al.* 1987) and galactic magnetic fields (Vachaspati 1992b). It can also provide large scale peculiar velocities (Vachaspati 1992a; Perivolaropoulos & Vachaspati 1994) and is consistent with the amplitude, spectral index (Bouchet, Bennett & Stebbins 1988; Bennett, Stebbins & Bouchet 1992; Perivolaropoulos 1993a) and the statistics (Gott *et. al.* 1990; Perivolaropoulos 1993b; Moessner, Perivolaropoulos & Brandenberger 1994; Coulson *et. al.* 1994; Luo 1994; Magueijo 1995b) of the cosmic microwave background (CMB) anisotropies measured by the COBE collaboration (Smoot *et. al.* 1992; Wright *et. al.* 1992) on large angular scales ($\theta \sim 10^\circ$). Other planned CMB experiments (see e.g. MAP 1997, COBRAS/SAMBA 1997, see also the review by Scott *et. al.* 1995) of equally high quality but on smaller angular scales are expected to provide a wealth of information within the next few years.

The CMB observations provide a valuable direct probe for identifying signatures of cosmic strings. The main mechanism by which strings can produce CMB fluctuations on angular scales larger than 1-2 degrees has been well studied both analytically (Brandenberger & Turok 1986; Stebbins 1988; Veeraraghavan & Stebbins 1990; Perivolaropoulos 1993a; Perivolaropoulos 1993b; Moessner *et. al.* 1994) and using numerical simulations (Bouchet *et.al.* 1988; Bennett *et. al.* 1992) and is known as the *Kaiser-Stebbins effect* (Kaiser &

(Stebbins 1984; Gott 1985). According to this effect, moving long strings present between the time of recombination t_{rec} and the present time t_0 , produce step-like temperature discontinuities between photons that reach the observer through opposite sides of the string. These discontinuities are due to the peculiar nature of the spacetime around a long string which even though is *locally* flat, *globally* has the geometry of a cone with deficit angle $8\pi G\mu$. The magnitude of the discontinuity is proportional to the deficit angle, to the string velocity v_s and depends on the relative orientation between the unit vector along the string \hat{s} and the unit photon wave-vector \hat{k} . It is given by (Stebbins 1988)

$$\frac{\delta T}{T} = \pm 4\pi G\mu v_s \gamma_s \hat{k} \cdot (\hat{v}_s \times \hat{s}) \quad (1)$$

where γ_s is the relativistic Lorentz factor and the sign changes when the string is crossed. The angular scale over which this discontinuity persists is given by the radius of curvature of the string which according to simulations (Bennett & Bouchet 1988; Allen & Shellard 1990; Albrecht & Stebbins 1993) is approximately equal to the horizon scale. The growth of the horizon from t_{rec} to t_0 results in a superposition of a large number of step-like temperature seeds of all sizes starting from about 2° (the angular size of the horizon at t_{rec}) to about 180° (the present horizon scale). By the central limit theorem this large number of superposed seeds results in a pattern of fluctuations that obeys Gaussian statistics. Thus the probability distribution for the temperature of each pixel of a CMB map with resolution larger than about $1^\circ - 2^\circ$ is a Gaussian (Allen et. al. 1996, Coulson et. al. 1994, Perivolaropoulos 1993b; Perivolaropoulos 1993c). It has therefore been considered to be impossible to distinguish structure formation models based on cosmic strings from corresponding models based on inflation, using CMB maps with resolution angle larger than $1^\circ - 2^\circ$ (Ferreira & Magueijo 1997). Theoretical studies have therefore focused on identifying the statistical signatures of cosmic strings on angular scales less than 1° (Turok 1996, Coulson et. al. 1994) where the number of superposed seeds is smaller and therefore

the non-Gaussian character of fluctuations is expected to be stronger ¹

These efforts however have been faced with the complicated and model dependent physical processes occurring on small angular scales. Such effects include isolated foreground point sources, recombination physics, string properties on small scales (kinks, loops etc) which require detailed simulations of both the string network and the cosmic background, in order to be properly taken into account. Even though preliminary efforts for such detailed simulations are in progress (Allen et. al. 1996), it has become clear that it will take some time before theory and experiments on angular scales less than a few arcmin reach accuracy levels leading to detectable non-Gaussian string signatures.

An alternative approach to the problem is instead of focusing on small scales where the number of superposed seeds is small, to focus on larger angular scales where despite the large number of superposed seeds there is also coherence of induced fluctuations on large angular scales. Fluctuations on these scales may be viewed as a superposition of a Gaussian scale invariant background coming mainly from small scale seeds plus a small number of step-like discontinuities which are coherent and persist on angular scales larger than 100° . These are produced by long strings present in our present horizon. *Our goal is to find a statistic optimized to detect this large scale coherence and use it to find the minimum amplitude of a step function that can be detected at the 1σ level relatively to a given scale invariant Gaussian background.* Such a statistic is equally effective on any angular resolution scale and its effectiveness is only diminished as the number of pixels of the CMB map is reduced or the noise is increased. The statistical variable we focus on, in what follows is the Sample Mean Difference (SMD) between large neighbouring sectors of a

¹The non-Gaussian features for texture maps are stronger than those of cosmic strings mainly because of the generically smaller number of textures per horizon volume (Gangui 1996; Magueijo 1995a).

CMB map. These sectors are separated by a random straight line in two dimensional maps or by a random point in one dimensional maps. The union of the two sectors gives back the complete map. We show that the statistics of the SMD variable are much more sensitive in detecting the presence of a coherent step-like seed than conventional statistics like the skewness or the kurtosis.

The structure of this paper is the following: In the next section titled 'Sample Mean Difference' we study analytically the statistics of the SMD variable and show that its average value is a sensitive quantity in detecting the presence of a randomly positioned step-function on top of a gaussian map. We then compare with the sensitivity of the statistics *skewness* and *kurtosis*. We find that the sensitivity of the SMD statistics is significantly superior to that of skewness and kurtosis in detecting the step function. These analytical results are shown for the case of one-dimensional maps but the extension to the case of two dimensional maps is straightforward.

In the third section titled 'Monte Carlo Simulations' we perform Monte Carlo simulations of Gaussian maps with flat and scale invariant power spectra, with and without step-like discontinuities in one and two dimensions. We also include noise with signal to noise ration $\frac{s}{n} = 1.0$. Applying the statistics skewness, kurtosis and average of SMD on these maps we verify the results of section 2 and find the minimum step-function amplitude that is detectable by the average SMD statistic. Finally in section 4 we conclude, summarise and discuss the prospect of applying the mean of SMD statistic to presently available CMB maps including the COBE results. That analysis is currently in progress (Athanasίου, Perivolaropoulos & Simatos 1997).

2. Sample Mean Difference

Consider an one dimensional array of n pixel variables x_n . Let these variables be initially distributed according to a standardised Gaussian probability distribution. Consider now a step-function of amplitude 2α superposed so that the discontinuity is between pixels i_0 and $i_0 + 1$ (Fig. 1). The new probability distribution for a random pixel variable x is

$$P(x) = \frac{f}{\sqrt{2\pi}} e^{-\frac{(x-\alpha)^2}{2}} + \frac{1-f}{\sqrt{2\pi}} e^{-\frac{(x+\alpha)^2}{2}} \quad (2)$$

where $f = \frac{i_0}{n}$. We are looking for a statistic that will optimally distinguish between a Gaussian array with a superposed step-function and a Gaussian array without one. The obvious statistics to try first are the moments of the distribution (2) with $\alpha = 0$ and $\alpha \neq 0$.

The moment generating function corresponding to (2) is:

$$M(t) = f e^{\alpha t + \frac{t^2}{2}} + (1-f) e^{-\alpha t + \frac{t^2}{2}} \quad (3)$$

The mean $\mu(\alpha, f)$, variance $\sigma^2(\alpha, f)$, skewness $s(\alpha, f)$ and kurtosis $k(\alpha, f)$ can be obtained in a straightforward way by proper differentiation of $M(t)$ as follows:

$$\mu(\alpha, f) \equiv \langle X \rangle = \alpha f - \alpha(1-f) \quad (4)$$

$$\sigma^2(\alpha, f) \equiv \langle (x - \mu)^2 \rangle = 1 + 4\alpha^2 f(1-f) \quad (5)$$

$$s(\alpha, f) \equiv \frac{\langle (x - \mu)^3 \rangle}{\sigma^3} = \frac{8\alpha^3 f(1-3f+2f^2)}{(1+4\alpha^2 f(1-f))^{3/2}} \quad (6)$$

$$\begin{aligned} k(\alpha, f) &\equiv \frac{\langle (x - \mu)^4 \rangle}{\sigma^4} \\ &= \frac{3 + 8\alpha^2 f(3 + 2\alpha^2 - 3f^2 - 8\alpha^2 f + 12\alpha^2 f^2 - 6\alpha^2 f^3)}{(1 + 4\alpha^2 f(1-f))^4} \end{aligned}$$

For $\alpha = 0$ we obtain the Gaussian values for the skewness and the kurtosis $s(0, f) = 0$, $k(0, f) = 3$ as expected. For $\alpha \neq 0$ the moments deviate from the Gaussian values. In order to find the minimum value of α for which the moments can distinguish between a

Gaussian pattern and a Gaussian+Step pattern we must compare the deviation of moments from their Gaussian values with the standard deviation of the sample moments. The mean values of the skewness and the kurtosis are easily obtained by integrating with respect to f from 0 to 1 i.e. assuming that it is equally probable for the step-function to be superposed at any point of the lattice.

$$\bar{s}(\alpha) = \langle s(\alpha, f) \rangle = \int_0^1 df s(\alpha, f) = 0 \quad (7)$$

$$\bar{k}(\alpha) = \langle k(\alpha, f) \rangle = \int_0^1 df k(\alpha, f) \quad (8)$$

These values are to be compared with the standard deviations of the moments, obtained as follows: The variance of the skewness over several n -pixel array realizations with fixed f and α is

$$\Delta s^2(\alpha, f) = \langle (\hat{s} - s)^2 \rangle \quad (9)$$

where $\hat{s} \equiv \frac{s_1 + \dots + s_n}{n}$ is the sample skewness from a given pixel array realization, s is the actual skewness and $s_i \equiv \frac{(x_i - \mu)^3}{\sigma^3}$. Now

$$\langle \hat{s} \rangle = \frac{n \langle s_1 \rangle}{n} = \langle s_1 \rangle = s \quad (10)$$

Also

$$\langle \hat{s}^2 \rangle = \frac{1}{n} \langle s_j^2 \rangle + \left(1 - \frac{1}{n}\right) \langle s_j \rangle^2 \quad (11)$$

where j any pixel number ($j \in [1, n]$). Thus

$$\Delta s^2(\alpha, f) = \frac{1}{n} (\langle s_j^2 \rangle - \langle s_j \rangle^2) = \frac{1}{n} \frac{1}{\sigma^6} \langle (x_j - \mu)^6 \rangle \quad (12)$$

Similarly for the variance of the sample kurtosis we have

$$\Delta k^2(\alpha, f) = \frac{1}{n} (\langle k_j^2 \rangle - \langle k_j \rangle^2) \quad (13)$$

with $k_j = \frac{1}{\sigma^4} (x_j - \mu)^4$ and $\langle k_j^2 \rangle = \frac{1}{\sigma^8} \langle (x_j - \mu)^8 \rangle$. It is straightforward to obtain all the above moments by differentiating the generating functional and using

$$\langle x_j^n \rangle = \frac{d^n M}{dt^n} \Big|_{t=0} \quad (14)$$

Now the minimum value α_{min} of α detectable at 1σ level is obtained from the equations

$$\int_0^1 df [s(\alpha_{min}, f) - \Delta s(\alpha_{min}, f)] = 0 \quad (15)$$

$$\int_0^1 df [(k(\alpha_{min}, f) - 3) - \Delta k(\alpha_{min}, f)] = 0 \quad (16)$$

Since (from eq. (7)) $\bar{s}(\alpha) = 0$ which is equal to the Gaussian value, the skewness can only be used to detect a step function by comparing the standard deviation $\Delta\bar{s}$ for $\alpha = 0$ and $\alpha \neq 0$. By demanding $\Delta\bar{s}(\alpha_{min}) \leq 2\Delta\bar{s}(\alpha = 0)$ we obtain $\alpha_{min} \leq 2.5$. This result is independent of the number of pixels n . For the kurtosis we obtain from eqs. (13, 16) $\alpha_{min} \simeq 4$ for $n = 10^3$ while for $\alpha_{min} = 0.5$, $n \simeq 10^6$ is required.

Using the alternative test i.e. demanding $\Delta\bar{k}(\alpha_{min}) \geq 2\Delta\bar{k}(\alpha = 0)$ we obtain $\alpha \geq 2$ and this result is independent of the number of pixels n as in the case of skewness. Thus for the usual pixel maps where n is up to $O(1000)$ the kurtosis is not able to detect a step function with $\alpha \leq 2$ at the 1σ level. As in all cases discussed in this paper α is measured in units of standard deviation (rms) of the underlying Gaussian map. This result remains unchanged for other statistical variables defined by *local* linear combinations of pixels (e.g. differences of neighbouring pixel variables (Moessner et. al. 1994, Coulson et. al. 1994)) since the effect of a single discontinuity remains negligible if the long range coherence is not taken into account.

For CMB temperature maps with $(\frac{\delta T}{T})_{rms} \simeq 2 \times 10^{-5}$ the detectable value of $G\mu$ is

$$\alpha \equiv 4\pi G\mu(v_s\gamma_s) \cos\theta > 4 \times 10^{-5} \Rightarrow G\mu(v_s\gamma_s) \cos\theta \geq 4 \times 10^{-6} \quad (17)$$

where θ is an angle obtained from the relative orientation of the string with respect to the observer. According to simulations $\langle v_s\gamma_s \rangle_{rms} \simeq 0.2$ and for $G\mu < 2 \times 10^{-5}$ the detection of the Kaiser-Stebbins effect using statistics based on skewness and kurtosis is not possible. This excluded range however includes all the cosmologically interesting values of $G\mu$.

It is therefore important to look for alternative statistical variables that are more

sensitive in detecting the presence of coherent discontinuities superposed on Gaussian maps. As we will show, the Sample Mean Difference (SMD) is such a statistical variable.

Consider a pixel array (Fig. 1) of n pixel Gaussian random variables X_j with a step function covering the whole array, superposed such that the discontinuity is located just after pixel i_0 . To every pixel k of the array we may associate the random variable Y_k defined as the difference between the mean value of the pixels 1 through k minus the mean value of the pixels $k + 1$ through n . It is straightforward to show that

$$Y_k = \Delta \bar{X}_k + 2\alpha \frac{n - i_0}{n - k} \quad k \in [1, i_0] \quad (18)$$

$$Y_k = \Delta \bar{X}_k + 2\alpha \frac{i_0}{k} \quad k \in [i_0, n - 1] \quad (19)$$

where $\Delta \bar{X}_k = \frac{1}{k} \sum_{j=1}^k X_j - \frac{1}{n-k} \sum_{j=k+1}^n X_j$. Thus we have constructed a new array Y_k , ($k = 1, \dots, n - 1$) from the sample mean differences (SMD) of the original array. We will focus on the average value Z of the SMD defined as:

$$Z = \frac{1}{n - 1} \sum_{k=1}^{n-1} Y_k \quad (20)$$

Using eqs. (19,20) we obtain

$$Z = \frac{1}{n - 1} \left[\sum_{k=1}^{n-1} \Delta \bar{X}_k + 2\alpha \left(\sum_{k=1}^{i_0} \frac{1 - i_0/n}{1 - k/n} + \sum_{k=i_0+1}^{n-1} \frac{i_0/n}{k/n} \right) \right] \quad (21)$$

With the definitions $f \equiv i_0/n$ and $\xi \equiv k/n$ and the assumption $n \gg 1$ we obtain:

$$Z = \frac{1}{n - 1} \sum_{k=1}^{n-1} \Delta \bar{X}_k - 2\alpha [(1 - f) \ln(1 - f) + f \ln f] \quad (22)$$

Thus the mean of Z over many realizations of the array is

$$\langle Z \rangle = \frac{1}{n - 1} \sum_{k=1}^{n-1} \langle \Delta \bar{X}_k \rangle - 4\alpha \left[\int_0^1 df f \ln f \right] = \alpha \quad (23)$$

The variance of Z is due both to the underlying Gaussian map and to the variation of $f = i_0/n$ (assuming α fixed). The variance due to the gaussian background is

$$\sigma_{1,Z} = \frac{1}{(n - 1)^2} \sum_{k=1}^{n-1} \left(\frac{1}{k} + \frac{1}{n - k} \right) \simeq \epsilon \int_{\epsilon}^{1-\epsilon} \frac{d\xi}{\xi(1 - \xi)} \quad (24)$$

where $\epsilon = O(\frac{1}{n})$, $\xi = k/n$, $n \gg 1$ and we have used the fact that the variance of the sample mean of a standardized Gaussian population with size j is $\frac{1}{j}$. Now from eq. (24) we obtain

$$\sigma_{1,Z}^2 \simeq -\epsilon \ln \epsilon^2 \simeq \frac{2 \ln n}{n} \quad (25)$$

The variance of the f -dependent part of Z is

$$\sigma_{2,Z} = \langle Z_2^2 \rangle - \langle Z_2 \rangle^2 \quad (26)$$

where $Z_2 \equiv -2\alpha[(1-f) \ln(1-f) + f \ln f]$. From eq. (23) we have $\langle Z_2 \rangle = \alpha$ and $\langle Z_2^2 \rangle$ is easily obtained as

$$\langle Z_2^2 \rangle = \int_0^1 df Z_2^2(f) \simeq \frac{4}{3} \alpha^2 \quad (27)$$

Thus

$$\sigma_Z^2 \equiv \sigma_{1,Z}^2 + \sigma_{2,Z}^2 = \frac{2 \ln n}{n} + \frac{1}{3} \alpha^2 \quad (28)$$

In order to be able to distinguish between a Gaussian+Step map and a purely Gaussian one, at the 1σ level we demand that

$$\langle Z \rangle_{\alpha \neq 0} - \langle Z \rangle_{\alpha=0} \geq \sigma_Z \quad (29)$$

This implies that the minimum value of α , α_{min} that can be detected using this test is

$$\alpha_{min} = \left(\frac{3 \ln n}{n} \right)^{1/2} \quad (30)$$

and for $n = O(10^3)$ we obtain $\alpha_{min} \simeq 0.2$ which is about an order of magnitude improvement over the corresponding sensitivity of tests based on the moments skewness and kurtosis. The reason for this significant improvement is the fact that the SMD statistical variable picks up the *coherence* properties introduced by the step function on the Gaussian map. The moments on the other hand pick up only local properties of the pixels and do not amplify the long range coherence of the step-like discontinuity.

Our analysis so far has assumed that the Gaussian variables X_j are independent and that the only correlation is introduced by the superposed step-function. In a realistic

setup however the underlying Gaussian map will be scale invariant and thus there will be correlations among the pixels. These correlations will also be affected by the instrument noise. In addition, our analysis has been limited so far to one dimensional maps while most CMB experiments are now obtaining two-dimensional maps. In order to take all these effects into account we need to apply the statistics of the SMD variable onto maps constructed by Monte Carlo simulations. This is the focus of the following section.

3. Monte-Carlo Simulations

We start by constructing an array of n Gaussian random variables X_j , $j = 1, \dots, n$ with a power spectrum $P(k) = k^{-m}$. Thus the values X_j associated with the pixel j is obtained as the Fourier transform of a function $g(k)$ ($k = 1, \dots, n$) with the following properties:

- For each k , the amplitude $|g(k)|$ is an independent random variable with 0 mean and variance $P(k) = 1/k^m$.
- The phase θ_k of each Fourier component $g(k)$ is an independent random variable in the range $[0, 2\pi]$ with uniform probability distribution $P(\theta_k) = \frac{1}{2\pi}$.
- The Fourier components are related by complex conjugation relations needed to give a *real* variable X_j .

The discrete Fourier transform definition used is

$$X_j = \frac{1}{\sqrt{n}} \sum_{k=1}^n g(k) e^{2\pi i (k-1)(j-1)/n} \quad (31)$$

and the numerical programming was implemented using *Mathematica* (Wolfram 1991). In order to have real X_j , the conditions

$$\text{Im}(0) = 0 \quad (32)$$

$$g(k+2) = g^*(n-k) \quad k = 0, \dots, n-2 \quad (33)$$

$$\text{Im}g\left(\frac{n}{2}+1\right) = 0 \quad (34)$$

must be satisfied. The array X_j obtained in the way described above is then standardized to a new array X_j^s , with

$$X_j^s \equiv \frac{(X_j - \mu)}{\sigma^2} \quad (35)$$

where μ and σ^2 are the sample mean and sample variance for the realization of the array X_j . A new array X'_j is then constructed by superposing to the array X_j^s a step function of amplitude 2α with discontinuity at a random point i_0 . The array X'_j is thus obtained as

$$X'_j = X_j^s + \alpha \frac{j - i_0}{|j - i_0|}, \quad j = 1, \dots, n \quad (36)$$

Next we apply the statistics discussed in the previous section to several realizations of the arrays X_j^s and X' in an effort to find the most sensitive statistic that can distinguish among them. Our goal is to also find the minimum value of α that can be distinguished by that statistic at the 1σ level, thus testing the analytical results of the previous section.

We have used a lattice with 2000 pixels and a scale invariant power spectrum which for one-dimensional data is $P(k) = k^{-1}$. In Table 1 we show the results for the skewness, the kurtosis and the average SMD for the X_j arrays, with $\alpha = 0, 0.25, 0.50$ and 1.0 . The SMD average was obtained as in section 2 by first constructing the array of sample mean differences and then obtaining its average value, predicted to be equal to α by the analytical study of section 2.

These statistics were applied to 50 random realizations of the array X_j^s . The mean values of the statistics considered with their 1σ standard deviations obtained over these 50 realizations are shown in the following Table 1.

Table 1: A comparison of the effectiveness of the statistics considered, in detecting the presence of a coherent step discontinuity with amplitude 2α relative to the standard deviation of the underlying Gaussian map. No noise was included in these simulations and the full map was used in obtaining the SMD average.

α	Skewness	Kurtosis	SMD Average
0.00	0.01 ± 0.11	2.97 ± 0.19	0.02 ± 0.31
0.25	0.01 ± 0.11	2.95 ± 0.20	0.25 ± 0.33
0.50	0.02 ± 0.11	2.88 ± 0.21	0.48 ± 0.38
1.00	0.03 ± 0.20	2.82 ± 0.32	0.98 ± 0.48

The analytical prediction of section 2 for the SMD average value α is in good agreement with the results of the Monte Carlo simulations. The standard deviation of this result is not in such a good agreement with the analytical prediction because the assumption of complete independence among pixels made by the analytical treatment is not realized in the Monte Carlo simulations where a scale invariant spectrum was considered and thus there was a non-trivial correlation among the pixels of the arrays.

The effects of adding uncorrelated Gaussian noise with signal to noise ratio $\frac{s}{n} = 1$ are shown in Table 2. This table was constructed by adding an uncorrelated Gaussian signal of unit variance to the standardized forms of the arrays X_j^s and X_j' and then repeating the statistics of Table 1.

From the results of Table 2 it becomes clear that the effects of noise do not affect significantly the sensitivity of the SMD average in detecting the presence of the coherent step.

Table 2: Similar to Table 1 but including noise in the Monte Carlo simulations with signal to noise ratio $\frac{s}{n} = 1.0$. The full map was used in obtaining the SMD average.

α	Skewness	Kurtosis	SMD Average
0.00	0.01 ± 0.10	2.97 ± 0.15	0.04 ± 0.31
0.25	0.01 ± 0.09	2.98 ± 0.13	0.21 ± 0.34
0.50	0.02 ± 0.08	2.98 ± 0.14	0.42 ± 0.39
1.00	0.01 ± 0.10	2.92 ± 0.14	0.97 ± 0.53

A simple way to further improve the sensitivity of the SMD statistical variable is to ignore a number l of boundary pixels of the SMD array, thus constructing its average using the Sample Mean Differences of pixels $l + 1, \dots, n - l$. From eq (24), the variance of the SMD for these pixels is significantly lower than the corresponding variance of the $2l$ pixels close to the boundaries. In addition, if the step is located within the central $n - 2l$ pixels the SMD average may be shown to be larger than α thus further amplifying the step signature. For $l = 150$ the variance of the SMD average *is reduced* by about 20% (Table 3) while the SMD average is *increased* by about 20% thus allowing the detection of steps as low as $\alpha = 0.25$ at the 1σ level. The price to pay for this sensitivity improvement is the reduction of the effective pixel area where the search for steps is made.

We have also used the SMD statistical variable for non-scale invariant power spectra and found that it works better for $P(k) = k^{-m}$ with $0 \leq m < 1$ than for $m > 1$. This is to be expected because large values of m imply larger correlations among pixels which in turn leads to a smaller number of effectively independent pixels and thus a larger value for the variance of the SMD average.

Table 3: Similar to Table 1 but the SMD average was obtained after ignoring 150 pixels on each boundary of the Monte Carlo maps. The discontinuities were also excluded from these 300 pixels. This significantly improved the sensitivity of the SMD test.

α	Skewness	Kurtosis	SMD Average
0.00	0.01 ± 0.10	2.96 ± 0.15	0.01 ± 0.24
0.25	0.01 ± 0.09	2.95 ± 0.15	0.28 ± 0.26
0.50	0.02 ± 0.14	2.94 ± 0.18	0.63 ± 0.29
1.00	0.03 ± 0.30	2.78 ± 0.30	1.21 ± 0.46

It is straightforward to generalize the one dimensional Monte Carlo simulations to two dimensions. In that case we use the two-dimensional discrete Fourier transform as an approximation to an expansion to spherical harmonics. This approximation is good for small area maps of the celestial sphere. We used the following definition of the two dimensional discrete Fourier transform.

$$X(i, j) = \frac{1}{n} \sum_{k_1=1}^n \sum_{k_2=1}^n g(k_1, k_2) e^{2\pi i[(i-1)(k_1-1)+(j-1)(k_2-1)]/n} \quad (37)$$

referring to a $n \times n$ square lattice. In order to construct the background of scale invariant Gaussian fluctuations we used $g(k_1, k_2)$ as a complex random variable. For scale invariance, the amplitude of $g(k_1, k_2)$ was obtained from a Gaussian probability distribution with 0 mean and variance

$$\sigma^2(k_1, k_2) = P(k_1, k_2) = \frac{1}{k_1^2 + k_2^2} \quad (38)$$

The corresponding phase θ_{k_1, k_2} for the (k_1, k_2) mode was also determined randomly from a uniform probability distribution $P(\theta_{k_1, k_2}) = \frac{1}{2\pi}$ in order to secure Gaussianity for the map $X(i, j)$. To secure that the Fourier transformed map $X(i, j)$ consists of real numbers, the following constraints were imposed on the spectrum $g(k_1, k_2)$

$$Img(1, 1) = Img(\frac{n}{2} + 1, 1) =$$

$$\begin{aligned}
= \text{Img}(1, \frac{n}{2} + 1) &= \text{Img}(\frac{n}{2} + 1, \frac{n}{2} + 1) = 0 \\
g(n - i, 1) &= g^*(i + 2, 1), & i = 0, \dots, \frac{n}{2} - 2 \\
g(1, n - i) &= g^*(1, i + 2), & i = 0, \dots, \frac{n}{2} - 2 \\
g(i, j) &= g^*(n - i + 2, n - j + 2), & i = 2, \dots, \frac{n}{2} + 1, \\
&& j = 2, \dots, n
\end{aligned}$$

The corresponding map with a superposed coherent step discontinuity was obtained from the standardized Gaussian map $X^s(i, j)$ as

$$X'(i, j) = X^s(i, j) + \alpha \frac{j - a i - b}{|j - a i - b|} \quad (39)$$

where

$$a = \frac{y_2 - y_1}{x_2 - x_1} \quad (40)$$

$$b = y_1 - a x_1 \quad (41)$$

i.e. the line of step discontinuity $j = a i + b$ is determined by the two random points (x_1, y_1) and (x_2, y_2) of the map $X(i, j)$. The skewness and kurtosis of the two maps are obtained in the usual way. For example for the standardized Gaussian map $X^s(i, j)$ we have

$$s = \frac{1}{n^2} \sum_{i,j}^n X^s(i, j)^3 \quad (42)$$

$$k = \frac{1}{n^2} \sum_{i,j}^n X^s(i, j)^4 \quad (43)$$

The SMD statistical variables is obtained by considering a set of random straight lines bisecting the map and for each line taking the difference of the sample means from the two parts of the map. For example consider a line defined by the random points (x_1, y_1) and (x_2, y_2) of the map. The line equation is $j = a i + b$ with a, b obtained from eqs. (40) and (41). The SMD obtained from this line is

$$\text{SMD} = \frac{S_1}{n_1} - \frac{S_2}{n_2} \quad (44)$$

where

$$S_1 = \sum_{i=1}^n \sum_{j=Max[(a-i+b),1]}^n X^s(i, j) \quad (45)$$

$$S_2 = \sum_{i=1}^n \sum_{j=1}^{Min[(a-i+b),n]} X^s(i, j) \quad (46)$$

and n_1, n_2 are the corresponding numbers of terms in the sums. For a Step+Gaussian map, the discontinuity the index s get replaced by $'$.

The average and variance of the SMD is obtained by averaging over a large number of random test lines (a, b) and a large number of map realizations. The results of the application of the three statistics (skewness, kurtosis and SMD average) on 30×30 scale invariant Gaussian maps for various values of step amplitudes α are shown in Table 4. Uncorrelated Gaussian noise with signal to noise ratio $\frac{s}{n} = 2.0$ was also included. The random points defining the test lines were excluded from the outermost three rows and columns of the maps thus reducing somewhat the variance of the SMD average.

Table 4: A comparison of the effectiveness of the statistics considered in two dimensional maps. A signal to noise ratio of $\frac{s}{n} = 2.0$ was assumed in these maps. Points defining the line discontinuities were excluded from the three outermost rows and columns of the maps.

α	Skewness	Kurtosis	SMD Average
0.00	0.04 ± 0.13	3.00 ± 0.20	0.01 ± 0.03
0.25	0.02 ± 0.08	2.97 ± 0.13	0.14 ± 0.09
0.50	0.05 ± 0.14	2.91 ± 0.24	0.34 ± 0.19
1.00	0.02 ± 0.24	2.95 ± 0.30	0.56 ± 0.31

The results of Table 4 are in qualitative agreement with those of Tables 1-3 and with the analytical results valid for the one dimensional maps. Clearly the details of the

one dimensional analysis are not valid in the two dimensional case and so the agreement can not be quantitative. The results still indicate however that the SMD statistic is significantly more sensitive compared to conventional statistics for the detection of coherent discontinuities on CMB maps. This statistic can detect coherent discontinuities with minimum amplitude $\alpha_{min} \simeq 0.5$ at the 1σ to 2σ level where α is the amplitude relative to the standard deviation of the underlying scale invariant Gaussian map.

4. Conclusion-Outlook

It is straightforward to apply the statistic analyzed in this paper to realistic data of ongoing experiments. Consider for example a $n \times n$ pixel sector of the COBE map including n^2 pixels. Let also $(\frac{\delta T}{T})_{rms}$ be the *rms* temperature fluctuations of the sector under consideration. The presence of a late long string through this sector would have caused a temperature step-discontinuity coherent over the whole map, with magnitude α given by eq. (1). If the average of the SMD over this sector is found to be very close to 0 (more than 1σ away from the SMD average value for $\alpha = 0.5$), then we may conclude that

$$\frac{\alpha}{(\frac{\delta T}{T})_{rms}} \leq \frac{\alpha}{(\frac{\delta T}{T})_{rms}^g} \leq 0.5 \quad (47)$$

at the 1σ confidence level, where $(\frac{\delta T}{T})_{rms}^g$ is the *rms* value of the purely Gaussian part of the fluctuations which is clearly smaller than the total $(\frac{\delta T}{T})_{rms}$ which includes the step discontinuity. Thus

$$G\mu v_s \gamma_s \cos \theta \leq \frac{1}{8\pi} (\frac{\delta T}{T})_{rms} \quad (48)$$

where θ is an angle determined by the orientation of the string with respect to the observer. For example for $(\frac{\delta T}{T})_{rms} = 10^{-5}$ we obtain $G\mu v_s \gamma_s \cos \theta \leq 4 \times 10^{-7}$ at the 1σ level.

Thus using the SMD statistic which is optimized to detect coherent temperature discontinuities on top of Gaussian temperature maps we may obtain non-trivial upper or

even *lower* bounds on the values of $G\mu v_s \gamma_s$ which are highly robust and independent of the details of the string evolution and the resolution of the CMB maps. Application of this statistic on the COBE data is currently in progress (Athanasίου, Perivolaropoulos & Simatos 1997).

I wish to thank G. Athanasίου, T. Tomaras and N. Simatos for interesting discussions and for providing helpful comments after reading the paper. This work was supported by the Greek General Secretariat for Research and Technology under grants ΠΕΝΕΔ 1170/95 and 95ΕΔ1759 and by the EEC grants $CHRX - CT93 - 0340$ and $CHRX - CT94 - 0621$.

REFERENCES

- Allen B. & Shellard E. P. S. 1990, Phys.Rev.Lett. 64, 119.
- Allen B., Caldwell R., Shellard E. P. S., Stebbins A. & Veeraraghavan S. 1996, DAMTP R96/23, FERMILAB-Pub-96/265-A, WISC-MILW-96/21, astro-ph/9609038.
- Albrecht A. & Stebbins A. 1993. Phys. Rev. Lett. 69, 2615.
- Athanasίου, Perivolaropoulos L. & Simatos N. 1997, in preparation.
- Bardeen J., Steinhardt P. & M.Turner M. 1983, Phys.Rev. D28, 679.
- Bennett D. & Bouchet F. 1988, Phys.Rev.Lett. 60, 257.
- Bennett D., Stebbins A. & Bouchet F. 1992, Ap.J.(Lett.) 399, L5.
- Bouchet F. R., Bennett D. P. & Stebbins A. 1988, Nature 335, 410.
- Brandenberger R. 1992, 'Topological Defect Models of Structure Formation After the COBE Discovery of CMB Anisotropies', Brown preprint BROWN-HET-881 (1992), publ. in proc. of the International School of Astrophysics "D.Chalonge", 6-13 Sept.1992, Erice, Italy, ed. N.Sanchez (World Scientific, Singapore, 1993).
- Brandenberger R., Kaiser N., Shellard E. P. S., Turok N. 1987. Phys.Rev. D36, 335.
- Brandenberger R. & Turok N. 1986, Phys. Rev. D33, 2182.
- COBRAS/SAMBA 1997, Homepage:
<http://astro.estec.esa.nl/SA-general/Projects/Cobras/cobras.html>.
- Coulson D., Ferreira P., Graham P. & Turok N. 1994, Nature, 368, 27, hep-ph/9310322.
- Efstathiou G. 1989, in 'Physics of the Early Universe', SUSSP 36, 1989, ed. J.Peacock, A.Heavens & A.Davies (IOP Publ., Bristol, 1990).
- Ferreira P., Magueijo J. 1997, Phys.Rev. D55 3358.
- Gangui A. 1996, Phys. Rev. D54, 4750.

- Gott R. 1985, Ap. J. 288, 422.
- Gott J. *et. al.* 1990, Ap.J. 352, 1.
- Guth A. & Pi S. -Y. 1982, Phys.Rev.Lett. 49, 110.
- Hara T. & Miyoshi S. 1993, Ap. J. 405, 419.
- Hawking S. 1982, Phys.Lett. 115B, 295.
- Kaiser N. & Stebbins A. 1984, Nature 310, 391.
- Kibble T. W. B. 1976, J.Phys. A9, 1387.
- Luo X. 1994, Phys. Rev. D49, 3810.
- Magueijo J. 1995a, Phys.Rev. D52, 689.
- Magueijo J. 1995b, Phys.Rev. D52, 4361.
- MAP 1997, Homepage: <http://map.gsfc.nasa.gov>.
- Moessner R., Perivolaropoulos L. & Brandenberger R. 1994, Ap. J. 425,365, astro-ph/9310001.
- Perivolaropoulos L. 1994, Trieste HEP Cosmology, 204-270.
- Perivolaropoulos L. 1993a, Phys.Lett. B298, 305.
- Perivolaropoulos L. 1993b, Phys. Rev. D48, 1530.
- Perivolaropoulos L. 1993c, M.N.R.A.S., 267 529.
- Perivolaropoulos L. & Vachaspati T. 1994, Ap. J. Lett. 423, L77.
- Perivolaropoulos L., Brandenberger R. & Stebbins A. 1990, Phys.Rev. D41, 1764.
- Scott D., Silk J. & M.White 1995, Science 268, 829.
- Smoot G. *et. al.* 1992, (COBE), Ap. J. Lett. 396, L1.
- Starobinsky A. 1982, Phys.Lett. 117B, 175.

- Stebbins A. *et. al.* 1987, Ap. J. 322, 1.
- Stebbins A. 1988, Ap.J. 327, 584.
- Turok N. 1996, astro-ph/9606087.
- Turok N. 1989, Phys. Rev. Lett. 63, 2625.
- Vachaspati T. 1986, Phys. Rev. Lett. 57, 1655.
- Vachaspati T. 1992a, Phys.Lett. B282, 305.
- Vachaspati T. 1992b, Phys. Rev. D45, 3487.
- Vachaspati T. & Vilenkin A. 1991. Phys. Rev. Lett. 67, 1057-1061.
- Veeraraghavan S. & Stebbins A. 1990, Ap.J. 365, 37.
- Vilenkin A. 1981, Phys.Rev. D23, 852.
- Vilenkin A. 1985, Phys.Rep. 121, 263; Vilenkin A. & Shellard E.P.S. 1994, 'Cosmic Strings and Other Topological Defects', Cambridge U. Press.
- Vollick D. N. 1992, Phys. Rev. D45, 1884.
- Wright E. L. *et. al.* 1992, Ap. J. Lett. 396, L5.
- Wolfram S. 1991, *Mathematica version 2.0*, Addison-Wesley.

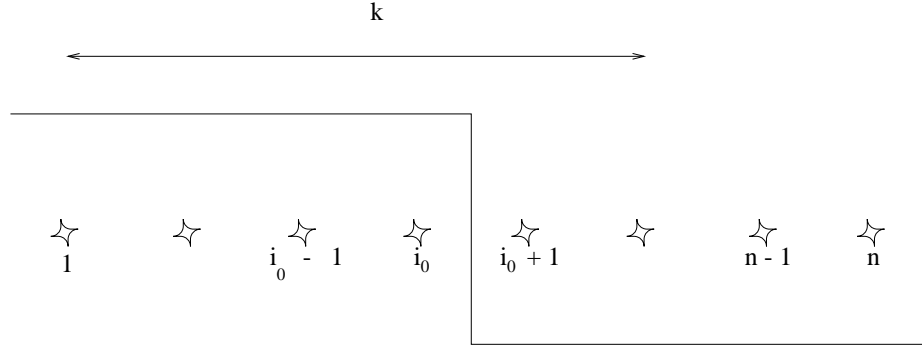


Fig. 1.— A large scale coherent step-function discontinuity superposed on a one dimensional pixel map.

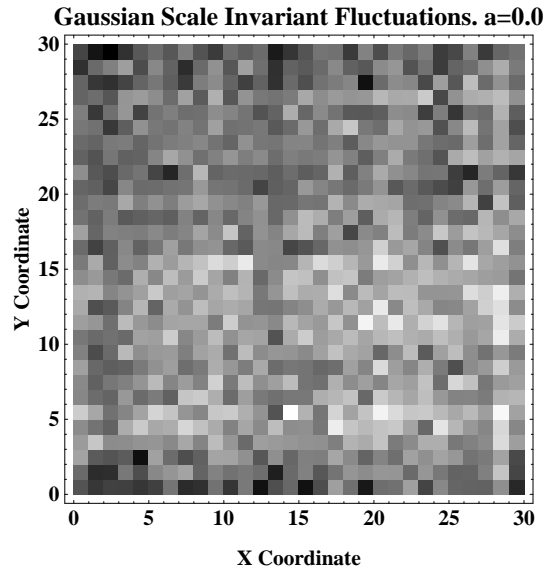


Fig. 2.— A standardized two dimensional pixel array of scale invariant Gaussian fluctuations. No step function has been superposed.

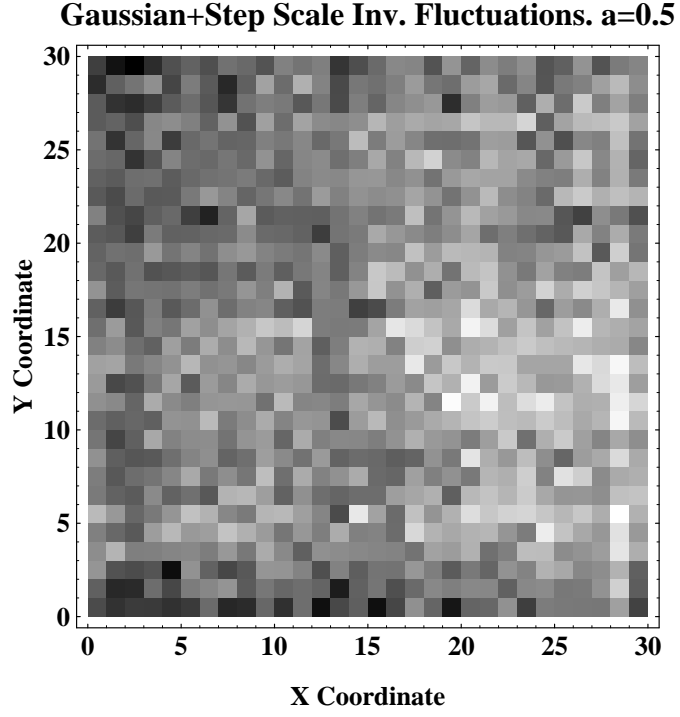


Fig. 3.— The two dimensional array of Figure 2 with a superposed coherent step-discontinuity of amplitude $\alpha = 0.5$ defined by the random points $(x_1, y_1) = (13.6, 18.1)$ and $(x_2, y_2) = (9.4, 20.4)$